TET-mediated epimutagenesis of the *Arabidopsis thaliana* methylome

Lexiang Ji[a,*], William T. Jordan[b,*], Xiuling Shi[b], Lulu Hu[c], Chuan He[c], Robert J. Schmitz[b]

[a]Institute of Bioinformatics, University of Georgia, Athens, GA, 30602, USA.

[b]Department of Genetics, University of Georgia, Athens, GA, 30602, USA.

[c]Department of Chemistry, Department of Biochemistry and Molecular Biology, and Institute for Biophysical Dynamics, Howard Hughes Medical Institute, University of Chicago, Chicago, IL 60637, USA

*Indicates these authors contributed equally to this work

Corresponding author:

Robert J. Schmitz

University of Georgia

120 East Green Street, Athens, GA 30602

Telephone: (706) 542-1887

Fax: (706) 542-3910

E-mail: schmitz@uga.edu

Keywords: DNA methylation, TET, epigenetics, epigenomics, epimutagenesis

DNA methylation in the promoters of plant genes sometimes leads to transcriptional repression, and the wholesale removal of DNA methylation as seen in methyltransferase mutants results in drastic changes in gene expression and severe developmental defects. However, many cases of naturally-occurring DNA methylation variations have been reported, whereby the altered expression of differentially methylated genes is responsible for agronomically important traits. The ability to manipulate plant methylomes to generate populations of epigenetically distinct individuals could provide invaluable resources for breeding and research purposes. Here we describe "epimutagenesis", a novel method to rapidly generate variation of DNA methylation through random demethylation of the *Arabidopsis thaliana* genome. This method involves the expression of a human Ten-eleven translocation (TET) enzyme, and results in widespread hypomethylation that can be inherited to subsequent generations, mimicking mutants in the maintenance DNA methyltransferase *met1*. Application of TET-mediated epimutagenesis to agriculturally significant plants may result in differential expression of alleles normally silenced by DNA methylation, uncovering previously hidden phenotypic variations.

Our ability to develop novel beneficial crop traits has significantly improved over the last 100 years, although the ability to maintain this trajectory is limited by allelic diversity. While genetic variation has been heavily exploited for crop improvement, utility of epigenetic variation has yet to be efficiently implemented. Epigenetic variation arises not from a change in the DNA sequence, but by changes in modifications to DNA such as cytosine methylation. This variation can result in emergence of novel and stably inherited phenotypes, as well as unique patterns of gene expression.

52 In plant genomes, cytosine methylation occurs at three major sequence contexts:
53 CG, CHG and CHH (where H = A, C or T)[1]. Methylation at these different contexts is
54 coordinated by distinct maintenance mechanisms during DNA replication. The
55 methylation of DNA in all three contexts is essential for transcriptional silencing of
56 transposons, repeat sequences and certain genes. Genes regulated by this mechanism
57 are stably repressed throughout the soma and represent an untapped source of hidden
58 genetic variation if transcriptionally re-activated, as revealed from pioneering studies in
59 the model plant *A. thaliana*[2, 3, 4]. However, the impact of this variation is not observed in
60 wild-type plants, as genes silenced by DNA methylation are not expressed. This novel
61 source of genetic variation was uncovered by creating epigenetic recombinant inbred
62 lines (epiRILs) from crosses between a wild-type individual and a mutant defective in
63 maintenance of DNA methylation[2, 3, 4]. EpiRILs, while genetically wild type, contain
64 mosaic DNA methylomes dependent on chromosomal inheritance patterns, as DNA
65 methylation is meiotically inherited in *A. thaliana*[2, 5, 6, 7, 8]. Phenotypic characterization of
66 epiRILs has revealed extensive morphological variation with respect to traits such as
67 flowering time, root length and resistance to bacterial infection[2, 3, 4]. The morphological
68 variation generated by the creation of epiRILs has revealed extensive hidden genetic
69 variation in plant genomes that can be observed due to expression of newly
70 unmethylated regions. However, the creation of epiRILs requires one founding parent to
71 be a null mutant in the maintenance DNA methylation pathway. Unfortunately, unlike in
72 *A. thaliana*, the loss of DNA methylation maintenance activity often results in lethality in
73 crops[9, 10]. Therefore, novel methodologies are required to realize the potential of these
74 hidden epialleles in crop genomes.
75 Epimutagenesis is an alternative method to generate epiRILs. Instead of relying
76 on the genome-wide demethylation of one of the two founding parents, epimutagenesis
77 introduces random methylation variation via the introduction of a transgene. Here, we

78 describe a novel epimutagenesis approach in *A. thaliana* using a human Ten-eleven
79 translocation (TET1) methylcytosine dioxygenase[11, 12, 13, 14], which catalyzes the
80 conversion of 5-methylcytosine (5mC) to 5-hydroxymethylcytosine (5hmC). Although
81 TET enzymes and their primary product 5hmC are not found in plant genomes[15], ectopic
82 expression of a human TET enzyme resulted in widespread DNA demethylation and
83 induced phenotypic variation in *A. thaliana*.
84
85 **RESULTS**
86 **Overexpressing hTET1cd in Arabidopsis hypomethylates the genome**
87 Transgenic *A. thaliana* plants were generated expressing the catalytic domain (residues
88 1418-2136) of the human TET1 protein (hTET1cd) under the control of the CaMV35S
89 promoter. To assess the impact of hTET1cd expression on the *A. thaliana* methylome,
90 whole genome bisulfite sequencing (WGBS) was performed on two independently
91 derived transgenic plants (35S:TET1-1 and 35S:TET1-2; **Supplementary Table 1**).
92 WGBS revealed a global reduction of CG methylation from 18.2% in two wild-type
93 individuals to 8.9% in 35S:TET1-1 and 6.9% in 35S:TET1-2 (compared to 0.5% in *met1-*
94 *3*). The effects of hTET1cd expression on CHG and CHH methylation were not as
95 severe compared to CG methylation (**Fig. 1a**). Importantly, different degrees of CG
96 hypomethylation were observed in different independent transgenic plants. This result
97 has important implications for epimutagenesis in economically and agriculturally
98 significant plant species, as it appears feasible to control the degree of DNA
99 hypomethylation by screening for plants with desired levels of demethylation. Taken
100 together, these results show that the expression of hTET1cd results in intermediate CG
101 methylation levels when compared to wild-type and *met1* individuals.
102 The primary product of TET1 oxidation is 5hmC, which is indistinguishable from
103 5mC by WGBS. We therefore performed Tet-assisted bisulfite sequencing (TAB-seq) to

104 profile 5hmC levels in 35S:TET1 plants[16]. No detectable levels of 5hmC were found in
105 the transgenic lines assayed (**Supplementary Fig. 1a-b)**. Thus, the widespread loss of
106 CG DNA methylation observed may result from a failure to maintain methylation at CG
107 sites that possess 5hmC, or through active removal of 5hmC or further oxidized products
108 via the base excision repair pathway.

109 To better understand the effects of hTET1cd expression, we determined changes
110 in the *A. thaliana* methylome at the chromosomal and local levels. Plotting methylation
111 levels across all five chromosomes revealed a strong depletion of CG methylation at the
112 pericentromeric region (**Fig. 1b**). CG hypomethylation occurred at both gene body
113 methylated (gbM) and select RNA-directed DNA methylated (RdDM) loci. (**Fig. 1c and**
114 **d**). To further quantify the observed hypomethylation, metaplots were created for genes
115 and transposons, respectively (**Fig. 1e and f, Supplementary Fig. 1c-f**). Strong
116 reduction of mCG and a mild reduction of mCHG/mCHH were observed at both genes
117 and transposons. On average, 97.9% of gbM genes and 56.7% of methylated
118 transposons (where these regions have at least 50% mCG in wild type) lost at least half
119 of their CG methylation in epimutagenized lines (**Supplementary Table 5 and 6**).
120 Collectively, these results indicate hypomethylation was more severe in genes than
121 transposons, possibly the result of *de novo* methylation by the RdDM pathway which is
122 primarily active at transposons.
123

124 **Tet1-mediated DNA demethylation mimics *met1* mutants**

125 An analysis of Differentially Methylated Regions (DMRs) was then carried out to assess
126 the genome-wide impact of hTET1cd expression. 56,283 CG DMRs ranging in size from
127 6 - 20,286 base pairs (bp) were identified (**Fig. 1g, Supplementary Table 7**). Of these,
128 38.7% were located in intergenic sequences, 53.7% overlapped with genes and 7.6%
129 were located in promoter regions (≤1kb upstream of a gene). As also seen in *met1*

130 mutants, the predominant effect of hTET1cd expression is CG hypomethylation (12,641
131 and 20,601 DMRs lost more than 50% mCG in 35S:TET1-1 and 35S:TET1-2,
132 respectively; no region gained more than 50% mCG). However, the extent of CG
133 methylation loss caused by hTETcd expression is lower than in *met1*: 31.8 Mb of the
134 genome significantly lost CG methylation in *met1*, whereas 9.9 Mb and 18.0 Mb were
135 lost in 35S:TET1-1 and 35S:TET1-2, respectively.

136 Previous studies of the *met1* methylome have revealed a loss of mCHG/mCHH
137 methylation in a subset of CG-hypomethylated regions [17]. At these loci, DNA methylation
138 is stably lost, in contrast to regions where DNA methylation is re-established by *de novo*
139 methylation pathways. These loci are ideal targets of epimutagenesis, as the co-
140 existence of all three types of methylation is more frequently correlated with
141 transcriptional repression of genes than CG methylation alone. This, coupled with the
142 long-term stability of hypomethylation, may facilitate inherited transcriptional changes.
143 An analysis of the interdependence of the loss of CG methylation on non-CG
144 methylation levels revealed that 39.7 Kb and 931.5 Kb of CHG methylated sequences
145 lost significant amounts of methylation in two independent epimutagenized lines,
146 compared to 4.0 Mb of sequence in *met1* mutants. A similar analysis for the loss of CHH
147 methylation revealed losses of 23.3 Kb and 492.5 Kb in epimutagenized individuals,
148 compared to 1.1 Mb lost in *met1* mutants. Of the 56,283 identified CG DMRs, 10,491
149 overlapped regions that contained at least 20% CHG methylation and 7,214 overlapped
150 regions that contained at least 10% CHH methylation in wild-type individuals
151 **(Supplementary Table 7)**. To determine how many of these regions are susceptible to
152 losing non-CG methylation if CG methylation is first depleted, we created a frequency
153 distribution of mCHG and mCHH levels in wild-type and epimutagenized individuals (**Fig.**
154 **1h and i**). 2,341 and 3,447 regions lost more than 10% CHG methylation in 35S:TET1-1
155 and 35S:TET1-2, respectively, whereas 2,475 and 3,379 regions lost more than 5%

156 CHH methylation in 35S:TET1-1 and 35S:TET1-2, respectively. Regions that are
157 susceptible to losses of CG and non-CG methylation in lines expressing hTET1cd share
158 a substantial overlap with regions that lose non-CG methylation in *met1*
159 (**Supplementary Fig. 1g and h)**. 1,708 (73.0%) and 2,386 (69.2%) regions that have
160 lost more than 10% mCHG in 35S:TET1-1 and 35S:TET1-2 have reduced levels in
161 *met1*, whereas 2,013 (81.6%) and 2,563 (75.9%) regions that have lost more than 5%
162 mCHH in 35S:TET1-1 and 35S:TET1-2 have reduced levels in *met1*. As crop genomes
163 have a greater number of loci targeted for silencing by CG, CHG and CHH methylation
164 when compared to *A. thaliana*, ectopic expression of hTET1cd is likely a viable approach
165 for the creation epiRILs[18].
166
167 **Tet1-mediated variation of CHG methylation**
168 Mutations in *met1* also result in hypermethylation of CHG sites in gene bodies due to the
169 loss of methylation in the 7th intron of the histone 3 lysine 9 (H3K9) demethylase,
170 *INCREASE IN BONSAI METHYLATION 1* (*IBM1*)[19, 20, 21, 22]. This results in alternative
171 splicing of *IBM1,* ultimately producing a non-functional gene product (IBM1-S), which
172 results in ectopic accumulation of di-methylation of H3K9 (H3K9me2) throughout the
173 genome[23]. As in *met1*, the 7th intron of *IBM1* was hypomethylated in 35S:TET1-1,
174 35S:TET1-2, and an additional two lines, 35S:TET1-2^{T5} and 35S:TET1-2^{T6}, which were
175 propagated for an additional two and three generations, respectively (**Fig. 2a**). The
176 increased abundance of *IBM1-S* and the reduction of functional *IBM1* (*IBM1-L)* transcript
177 was confirmed by RT-qPCR in line 35S:TET1-2^{T6} (**Supplementary Fig. 2a**) leading to
178 CHG hypermethylation at gbM loci (**Fig. 2b**). Further quantitative analysis revealed
179 extensive variation in genome-wide gains and losses of CHG methylation in these two
180 lines, approximately 1.8 Mb and 2.3 Mb of additional CHG methylation, respectively (**Fig.
181 2c, Supplementary Fig. 2b and c**). To test the impact of a reduction in functional *IBM1*

182 on H3K9me2, we performed chromatin immunoprecipitation (ChIP) against H3K9me2 in
183 35S:TET1-2^{T6}, which revealed a subtle increase in H3K9me2 in gbM loci that possessed
184 CHG hypermethylation (**Fig. 3d**).

185 To further characterize regions of differential CHG methylation, identified CHG
186 DMRs in line 35S:TET1-2^{T5} were categorized into discrete groups based on their DNA
187 methylation status in wild-type individuals. Of the 9,917 CHG DMRs identified, 1,460
188 were in loci that are defined as gbM in wild-type individuals, 584 were in unmethylated
189 regions, and 6,940 of them were in RdDM-like regions (**Fig. 2e-g**). Interestingly, in line
190 35S:TET1-2^{T5}, 1,408 (96.4%) of the CHG DMRs in gbM-like loci gained CHG
191 hypermethylation, whereas 2,156 (31.1%) of the CHG DMRs in RdDM-like regions lost
192 CHG, in contrast to 595 (8.6%) RdDM-like regions that gained CHG methylation. Lastly,
193 there were 502 (86.0%) loci that are unmethylated in wild-type individuals that gain CHG
194 methylation as well as CG and CHH methylation in the epimutagenized lines (**Fig. 2e-g**).
195 These results reveal that methods for epimutagenesis can result in both losses and
196 gains in DNA methylation genome-wide.

197 To characterize the effect of hTET1cd-induced methylome changes on gene
198 expression, we performed RNA-sequencing (RNA-seq) on leaf tissue of wild-type,
199 35S:TET1-1 and 35S:TET1-2. Compared to wild-type plants, 629 and 736 up-regulated
200 genes were identified in 35S:TET1-1 and 35S:TET1-2, respectively, with 176 and 260
201 genes overlapping with identified CG DMRs. 1,277 and 1,428 down-regulated genes
202 were identified and 268 and 324 of them overlapped with CG DMRs. There was a high
203 level of overlap in transcriptome changes seen in 35S:TET1-1 and 35S:TET1-2
204 compared to *met1* and *ibm1* (**Fig. 2h and i**). Of the genes up-regulated in *met1*, 36.8%
205 and 38.7% overlapped with up-regulated genes in 35S:TET1-1 and 35S:TET1-2,
206 respectively (**Supplementary Fig. 2d**). An even greater overlap was observed with
207 down-regulated genes in *met1*, as 60.1% and 65.2% overlapped with down-regulated

208 genes in 35S:TET1-1 and 35S:TET1-2, respectively (**Supplementary Fig. 2e**). These
209 results reveal that hTET1cd expression in *A. thaliana* is a viable approach for accessing
210 hidden sources of allelic variation by inducing expression variation.
211
212 **Tet1 expression leads to a delay in the floral transition**
213 In the transgenic plants that were used for WGBS, we observed a delay in the
214 developmental transition from vegetative to reproductive growth (**Fig. 3a and b**). We
215 hypothesized that the observed late-flowering phenotype was associated with the
216 demethylation of the *FWA* (*FLOWERING WAGENINGEN*) locus, as is observed in *met1*
217 mutants[24, 25]. A closer inspection of the DNA methylation status of this locus revealed
218 that DNA methylation was completely abolished, as was methylation at adjacent CHG
219 and CHH sites (**Fig. 3c**). As in *met1*, the loss of methylation at the *FWA* locus was
220 associated with an increase in *FWA* expression (**Fig. 3d**), which is known to cause a
221 delay in flowering by restricting the movement of the florigen signal*, FT*, to the shoot
222 apex[26]. These results demonstrate that expression of hTET1cd leads to phenotypic
223 variation by abolishing methylation at some regions in all sequence contexts (CG, CHG
224 and CHH sites).
225
226 **Tet1-mediated demethylation can be stably inherited over generations**
227 To assess the stability and inheritance of Tet1-mediated demethylation, T1 individuals
228 expressing 35S:TET1 were self-fertilized, allowing for the loss of the hTET1cd transgene
229 due to allelic segregation. Unexpectedly, transgene-free 35S:TET1-1 T2 individuals
230 (35S:TET1-1.3^{-TET1}, 35S:TET1-1.4^{-TET1} and 35S:TET1-1.5^{-TET1}) exhibited a reversion to a
231 normal flowering phenotype, and genome-wide methylation levels closely resembled that
232 of wild-type individuals (**Fig. 4a**). WGBS on T2 individuals retaining the transgene
233 revealed similar levels of CG methylation as the T1 parent (35S:TET1-1.1^{+TET1} and

234 35S:TET1-1.2^{+TET1}). The methylation level of CGs at genes and transposons revealed
235 that demethylation of gbM loci was partially inherited in transgene-free T2 individuals,
236 whereas active remethylation was found at transposons in the same individuals (**Fig. 4b-**
237 **f**). These results indicate that an active process likely in the meristem and/or germline is
238 counteracting the activity of the hTET1cd transgene[27]. To quantify how many regions
239 were susceptible to the loss of non-CG methylation, a DMR analysis was conducted for
240 each 35S:TET1-1 T2 individual. 655 and 659 CHG hypomethylated regions were
241 identified in T2 lines retaining the transgene. In contrast, 155, 199 and 201
242 hypomethylated regions were identified in three transgene-free T2 individuals,
243 respectively (**Fig. 4g**).
244 To determine if increased expression of hTET1cd would increase the likelihood
245 of germline transmittance of demethylation to transgene-free progeny, transgenic *A.*
246 *thaliana* plants were generated expressing a previously described superfolder GFP
247 (sfGFP) hTET1cd fusion, under control of the *A. thaliana* ACTIN 2 (ACT2) promoter
248 (ACT2:sfGFP-hTET1cd) which is known to have activity in all tissues of juvenile plants,
249 including meristematic tissue[28]. Translation and nuclear localization of the sfGFP-
250 TET1cd fusion protein was confirmed in young cotyledons using confocal microscopy
251 (**Supplementary Fig 3a**). T1 populations transformed with ACT2:sfGFP-hTET1cd
252 exhibited a 27-fold increase in later flowering compared to 35S:hTET1cd, indicating high
253 activity of the sfGFP-TET1cd fusion protein in *A. thaliana* (**Fig. 5a**). To assess the
254 variation between lines, we performed WGBS on four independent ACT2:TET1 T1 lines
255 (**Supplementary Fig. 4a-c**). Differential levels of global CG demethylation were
256 observed in these four lines, further confirming that plants subjected to epimutagenesis
257 can possess different degrees of demethylation. Subsequent DMR analysis revealed
258 68,260 CG DMRs, 9,235 CHG DMRs and 2,793 CHH DMRs between these lines, a
259 drastic increase in DMRs compared to those within siblings (**Fig. 4g**).

260 To further assess the inheritance of the demethylation pattern as a result of
261 epimutagenesis, we selected T2 progeny of a late flowering ACT2:TET1-1 T1 individual
262 containing and lacking the transgene. Individuals retaining and lacking the transgene
263 due to allelic segregation both exhibited a late-flowering phenotype, ectopic expression
264 and loss of DNA methylation of *FWA* (**Supplementary Fig 3b and c**). WGBS on these
265 two individuals revealed a reduction in CG methylation that was maintained and stably
266 inherited irrespective of transgene presence, confirming the high activity of
267 demethylation in ACT2:TET1 lines compared to 35S:TET1 lines (**Fig. 5b-f**). It is unclear
268 exactly why the late-flowering phenotype was stably inherited in the T2 individuals
269 without the transgene in the ACT2 driven lines versus the 35S driven lines, although it is
270 likely a combination of promoter strength and cell type specificity. For stable inheritance
271 of demethylation and the late-flowering phenotype TET1 activity would be required in the
272 meristematic and/or germline cells. Collectively, these results demonstrate the stable
273 inheritance of TET1-mediated demethylation and a delayed floral transition in the
274 absence of the transgene.
275
276 **DISCUSSION**
277 The discovery that expression of the catalytic domain of the human TET1 protein in *A.*
278 *thaliana* leads to widespread loss of CG methylation and enables the creation
279 epimutants without the need for methyltransferase mutants, which often causes lethality
280 in crops. In addition to epimutagenesis, hTET1cd could be used in combination with
281 sequence-specific DNA binding proteins such as dCas9 to direct DNA demethylation in
282 plant genomes, as has been demonstrated in mammalian systems[29, 30, 31, 32, 33]. The
283 stable meiotic inheritance of DNA methylation states in flowering plant genomes
284 provides a stark contrast to the inheritance of DNA methylation in mammalian genomes,
285 where genome-wide erasure of DNA methylation and reprogramming occurs each

generation[34]. This property of flowering plant genomes makes them ideal targets of induced-epialleles, as once a new methylation state occurs it is often inherited in subsequent generations. Application of epimutagenesis and the use of TET-mediated engineering of DNA methylation states in economically and agriculturally significant plant species will be an interesting area of future investigation.

ACKNOWLEDGEMENTS

We thank Nathan Springer for comments and discussions on this study as well as the Georgia Genomics Facility and the Georgia Advanced Computing Resource Center for technical support. This work was supported by the National Science Foundation (MCB-1650331), by The Pew Charitable Trusts and by the Office of the Vice President of Research at UGA to R.J.S. C.H was supported by the National Institutes of Health (NIH HG006827) and is an investigator of the Howard Hughes Medical Institute. W.T.J. was supported by a Scholars of Excellence Fellowship from the University of Georgia and National Institute of General Medical Sciences of the National Institutes of Health award number T32GM007103. The content is solely the responsibility of the authors and does not necessarily represent the official view of the National Institutes of Health.

AUTHOR CONTRIBUTIONS

R.J.S. conceived the project. L.J., W.T.J. and R.J.S. designed experiments. L.J., W.T.J., X.S., L.H., and C.H. performed research. L.J., W.T.J. and R.J.S. analyzed the data. R.J.S. wrote the paper. All authors discussed the results and commented on the manuscript.

COMPETING FINANCIAL INTERESTS

311 A provisional patent is pending for the development of this technology as it applies to
312 epigenome engineering of plants.
313
314
315 **Figure 1. Overexpression of hTET1cd induced global CG demethylation in *A.***
316 ***thaliana*.** (a) Bar graph of global methylation levels in two Col-0 WT replicates, two
317 35S:TET1 transgenic individuals and *met1*. (b) Metaplot of CG methylation levels (100
318 kb windows) across five *A. thaliana* chromosomes. Methylation level differences were
319 defined relative to Col-0 WT-1, and Col-0 WT-2 was used to assess background
320 interference. Genome browser view of methylome profile of two regions (c and d) of the
321 *A. thaliana* genome (purple vertical lines = CG methylation, blue vertical lines = CHG
322 methylation and gold vertical lines = CHH methylation). Metagene plots of CG
323 methylation level across (e) gene bodies and (f) transposable elements. (g) Heat map of
324 CG methylation level of CG DMRs. Bar plots of CHG (h) and CHH (i) methylation levels
325 of CG DMRs that possess non-CG methylation in wild-type individuals.
326
327 **Figure 2. Global fluctuation of CHG methylation in 35S:TET1 plants.** (a) Genome
328 browser view of *IBM1* (AT3G07610) in Col-0 WT, three 35S:TET1 transgenic plants and
329 *met1*. A decrease in CG methylation from coding regions was accompanied by an
330 increase in non-CG methylation. Both CG and non-CG methylation was lost from the
331 large intron (purple vertical lines = CG methylation, blue vertical lines = CHG methylation
332 and gold vertical lines = CHH methylation). (b) Genome browser view of a representative
333 CHG hypermethylated region. (c) The amount of the genome affected by differential
334 CHG methylation. These DMRs were defined relative to Col-0 WT-1, as Col-0 WT-2
335 DMRs were used to assess background interference. (d) Boxplot of H3K9me2
336 distribution in gbM loci (**, t-test, p-value < 0.01). (e) Heat map of CHG methylation

337 displaying CHG DMRs. Corresponding CG and CHH methylation levels are shown in (f)
338 and (g). Heat maps showing log_2 transformed FPKM profiles of up-regulated genes (h)
339 and down-regulated genes (i) in two 35S:TET1 transgenic individuals, *met1* and *ibm1*
340 mutants relative to WT.
341
342 **Figure 3. 35S:TET1 plants have a delayed flowering phenotype.** (a) Photographs of
343 one 35S:TET1-1 transgenic plant and Col-0 WT plant and (b) corresponding number of
344 rosette leaves (**, t-test, p-value < 0.01). (c) Genome browser view of *FWA*
345 (AT4G25530). Both CG and non-CG DNA methylation are depleted from the 5'UTR in
346 35S:TET1-2 plants (purple vertical lines = CG methylation, blue vertical lines = CHG
347 methylation and gold vertical lines = CHH methylation). (d) Expression level (FPKM) of
348 *FWA*.
349
350
351 **Figure 4. Transgenerational demethylation profile of 35S:TET1 individuals.** (a) Bar
352 plots of global methylation levels in two Col-0 WT replicates and 35S:TET1-1 plants.
353 Metagene plots of mCG level across (b) gene bodies and (c) transposable elements.
354 Heat map of mCG level of (d) all gbM genes and (e) transposable elements with >20%
355 mCG in wild type. (f) Genome browser view of a methylome profile of a representative
356 region of the *A. thaliana* genome in 35S:TET1-1 individuals. (g) Number of identified
357 CHG DMRs in ACT2:TET1 T2 plants. These DMRs were defined relative to Col-0 WT-1,
358 as Col-0 WT-2 DMRs were used to assess background.
359
360
361 **Figure 5. Demethylation profile of ACT2:TET1 individuals.** (a) Bar plot of number of
362 rosette leaves in 35S:TET1 and ACT2:TET1 T1 individuals upon flowering. (b) Bar plot
363 of global methylation levels in two Col-0 WT replicates and two ACT2:TET1-1 T2 plants.

364 Metagene plots of mCG level across (c) gene bodies and (d) transposable elements.
365 Heat map of mCG level of (e) all gbM genes and (f) transposable elements with >20%
366 mCG in wild type.
367
368 **METHODS**

369 **Synthesis and cloning of the human TET1 catalytic domain.** A human TET1 catalytic
370 domain (hTET1cd) sequence (residues 1418-2136) was synthesized by GenScript, and
371 moved to a plant transformation compatible vector (pMDC32) using LR clonase from Life
372 Technologies per the manufacturer's instructions (Catalog #11791100). ACT2:sfGFP-
373 hTET1cd was subcloned by Genscript in the pMDC32 vector background using the
374 sfGFP-TET1cd fragment from Addgene plasmid #82561. The ACT2 promoter sequence
375 was kindly provided by Dr. Richard Meagher.
376

377 **Plant transformation and screening.** The hTET1cd sequence in the pMDC32 vector
378 was transformed into *Agrobacterium tumefaciens* strain C58C1 and plated on LB-agar
379 supplemented with kanamycin (50 µg/mL), gentamicin (25 µg/mL), and rifampicin (50
380 µg/mL). A single kanamycin resistant colony was selected and used to start a 250-mL
381 culture in LB Broth Miller liquid media supplemented with gentamicin (25 µg/mL),
382 kanamycin (50 µg/mL), and rifampicin (50 µg/mL), which was incubated for two days at
383 30˚C. Bacterial cells were pelleted by centrifugation at 4,000 RPM for 30 minutes and
384 the supernatant decanted. The remaining bacterial pellet was re-suspended in 200 mL of
385 5% sucrose with 0.05% Silwet L77. Plant transformation was performed using the floral
386 dip method described by Clough and Bent[35]. Seeds were harvested upon senescence
387 and transgenic plants were identified via selection on ½ LS plates supplemented with
388 Hygromycin B (25 µg/mL). 35S:TET1-1 is a T1 individual, 35S:TET1-2 is a T3 plant,
389 35S:TET1-3 is a T4 plant. All transgenic individuals chosen for analysis contain

390 independent insertions of hTET1cd and are not the result of single-seed decent unless
391 otherwise noted.
392
393 **DNA and RNA isolation.** *A. thaliana* leaf tissue was flash-frozen and finely ground to a
394 powder using a mortar and pestle. DNA extraction was carried out on all samples using
395 the DNeasy Plant Mini Kit (QIAGEN), and the DNA was sheered to approximately 200
396 bp by sonication. RNA was isolated from finely ground flash-frozen leaf tissue using
397 Trizol (Thermo Scientific). For RT-qPCR, RNA was further treated with TURBO™
398 DNase (Thermo Scientific) according to manufacturers instructions. One µg of RNA was
399 subsequently reverse transcribed with M-MuLV Reverse Transcriptase according to
400 manufacturers instructions (NEB). RT-qPCR was used to analyzed cDNA populations
401 using PP2AA-3 (AT1G13320) as an endogenous control, and was performed on a
402 Roche LIghtCycler 480 instrument using SYBR Green detection chemistry. The genes
403 assayed by this method were *IBM1-S*, *IBM1-L,* and *FWA*. Primers used for RT-qPCR
404 were designed using PrimerQuest from Integrated DNA Technologies
405 (www.idtdna.com/PrimerQuest/). Primers sequences used for RT-qPCR: PP2A-F: 5'
406 AATGAGGCAGAAGTTCGGATAG 3', PP2A-R: 5'CAGGGAAGAATGTGCTGGATAG 3',
407 ibm1s-F: 5' TCTTTCTTCTAAGTCTGTCCATTCT 3', ibm1s-R: 5'
408 GTGACCGATTAGGAAATGGTATCT 3', ibm1L-F: 5' CCGAAGCCAAAGTGGAGATA 3',
409 ibm1L-R: 5' CTTCCTCTTCCGTAGACTTCTTT 3', FWA-F: 5'
410 CAAGATGGTGGAAGGATGAGAA 3', FWA-R: 5' CTCTGTTCTTCAGTGGGATGAG 3'.
411
412 **Library construction.** Genomic DNA libraries were prepared following the MethylC-seq
413 protocol without use of the bisulfite conversion step. MethylC-seq libraries were
414 prepared as previously described in[36]. RNA-seq libraries were constructed using Illumina
415 TruSeq Stranded RNA LT Kit (Illumina, San Diego, CA) following the manufacturer's

416 instructions with limited modifications. The starting quantity of total RNA was adjusted to
417 1.3 µg, and all volumes were reduced to a third of the described quantity. TAB-seq
418 libraries were prepared as previously described in[16].
419
420 **ChIP library preparation**. Leaves were treated with formaldehyde to covalently link
421 protein to DNA, washed several times with distilled water, patted dry and ground into fine
422 powder in liquid nitrogen. Chromatin was extracted with a series of extraction buffers
423 and sonicated. The final chromatin solution was incubated overnight with anti-H3K9me2
424 antibody (Cell Signaling Technology, 9753S) coated Dynabeads protein A (Life
425 Technologies, 10002D) to precipitate the immune complex. After a few washes, the
426 immune complex was eluted and incubated at 65 degrees in the presence of a high
427 concentration of NaCl in a water-bath overnight. After degrading the proteins with
428 proteinase K, DNA was recovered by phenol/chloroform/isoamyl alcohol extraction
429 followed by ethanol precipitation. The DNA pellet was then dissolved in 30µl of nuclease-
430 free water.
431
432 **Sequencing.** Illumina sequencing was performed at the University of Georgia Genomics
433 Facility using an Illumina NextSeq 500 instrument. For MethylC-seq and TAB-seq, raw
434 reads were trimmed for adapters and preprocessed to remove low quality reads using
435 cutadapt 1.9.dev1[37]. For RNA-seq and ChIP-seq, these processes were carried out by
436 Trimmomatic v0.32[38]. The mutant allele of *met1* is *met1-3* and methylome data was
437 downloaded under accession GSE39901. The mutant allele of *ibm1* is *ibm1-6*.
438
439 **MethylC-seq data processing.** Qualified reads were aligned to the *A. thaliana* TAIR10
440 reference genome as described in[39]. Chloroplast DNA (which is fully unmethylated) was
441 used as a control to calculate the sodium bisulfite reaction non-conversion rate of

442 unmodified cytosines. All conversion rates were >99% (**Supplementary Table 1**). The
443 list of gbM genes used in this study was previously curated[18]. Heat maps were clustered
444 by Complete Linkage method conducted by R (https://www.r-project.org). All methylation
445 levels reported in all analyses are presented as differences in absolute values, including
446 defining DMRs and calculating hyper/hypomethylated regions. The only exception is in
447 the comparison of mCG loss between gbM, where we used a percentage difference.
448
449 **RNA-seq data processing.** Qualified reads were aligned to the *A. thaliana* TAIR10
450 reference genome using TopHat v2.0.13[40] (**Supplementary Table 2**). Gene expression
451 values were computed using Cufflinks v2.2.1[41]. Genes determined to have at least 2-fold
452 $\log_2$ expression changes by Cufflinks and passed tests were identified as differentially
453 expressed genes.
454
455 **TAB-seq data processing.** Qualified reads were aligned to the *A. thaliana* TAIR10
456 reference genome using Methylpy as described in[39]. A modified lambda DNA sequence
457 was used to assess the quality of prepared libraries. In the added lambda sequence, all
458 non-CG cytosines are unmethylated and CG cytosines are methylated to 5mC. The
459 'non-conversion' rate is used to measure the rate of non-CG cytosines failing to be
460 converted to thymines after bisulfite treatment. The '5mC non-conversion' is used to
461 estimate the 5mCG cytosines failing to be converted to thymines after TET treatment.
462 (**Supplementary Table 3**).
463
464 **ChIP-Seq Data Analysis.** Qualified reads were aligned to the *A. thaliana* TAIR10
465 reference genome using Bowtie 1.1.1 with following parameters: bowtie -m 1 -v 2 --best -
466 -strata --chunkmbs 1024 -S. Aligned reads were sorted using samtools v 1.2 and clonal
467 duplicates were removed using SAMtools version 0.1.19 (**Supplementary Table 4**).

468

469 **Metaplot analysis.** For metaplot analyses, twenty 50 bp bins were created for both
470 upstream and downstream regions of gene bodies/TEs. Gene bodies/TE regions were
471 evenly divided into 20 bins. Weighted methylation levels were computed for each bin as
472 described previously[42].

473

474 **DMR analysis.** Identification of DMRs was performed as described in[43] and adjusted p-
475 value (Benjamini-Hochberg correction) 0.05 was adopted as the cutoff. Only DMRs with
476 at least 5 DMSs (Differential Methylated Sites) and a 10% absolute methylation level
477 difference within each DMR were reported and used for subsequent analysis. For
478 coverage calculations, each sample was combined with two Col-0 WT replicates to
479 identify DMRs. Each sample was compared with both Col-0 WT replicates separately
480 and for a DMR to be identified it must have been identified in both comparisons.
481 Absolute methylation differences of +/- (50% for CG, 10% for CHG and CHH) were
482 defined as hyper/hypo methylation, respectively. DMRs overlapping regions with mCG
483 >= 5%, mCHG and mCHH >= 1% in both two Col-0 WT replicates were defined as
484 RdDM-like regions. DMRs overlapping regions with mCG >= 5%, mCHG and mCHH <
485 1% in both two Col-0 WT replicates were defined as gbM regions. DMRs overlapping
486 regions with all three contexts less methylated at less than 1% in both Col-0 WT
487 replicates were defined as unmethylated regions. Overlap comparisons were performed
488 using bedtools v2.26.0[44].

489

490 **Data availability:** The data generated from this study has been uploaded to Gene
491 Expression Omnibus (GEO) database and can be retrieved through accession number
492 GSE93024.

493 **References**
494

495 1. Law JA, Jacobsen SE. Establishing, maintaining and modifying DNA
496 methylation patterns in plants and animals. *Nature reviews Genetics* **11**, 204-
497 220 (2010).
498
499 2. Johannes F*, et al.* Assessing the impact of transgenerational epigenetic
500 variation on complex traits. *PLoS Genet* **5**, e1000530 (2009).
501
502 3. Reinders J*, et al.* Compromised stability of DNA methylation and transposon
503 immobilization in mosaic Arabidopsis epigenomes. *Genes Dev* **23**, 939-950
504 (2009).
505
506 4. Cortijo S*, et al.* Mapping the Epigenetic Basis of Complex Traits. *Science*,
507 (2014).
508
509 5. Bewick AJ*, et al.* On the origin and evolutionary consequences of gene body
510 DNA methylation. *Proc Natl Acad Sci U S A* **113**, 9111-9116 (2016).
511
512 6. Cortijo S, Wardenaar R, Colome-Tatche M, Johannes F, Colot V. Genome-Wide
513 Analysis of DNA Methylation in Arabidopsis Using MeDIP-Chip. *Methods Mol*
514 *Biol* **1112**, 125-149 (2014).
515
516 7. Reinders J, Delucinge Vivier C, Theiler G, Chollet D, Descombes P, Paszkowski
517 J. Genome-wide, high-resolution DNA methylation profiling using bisulfite-
518 mediated cytosine conversion. *Genome Res* **18**, 469-476 (2008).
519
520 8. Hofmeister BT, Lee K, Rohr NA, Hall DW, Schmitz RJ. Stable inheritance of
521 DNA methylation allows creation of epigenotype maps and the study of
522 epiallele inheritance patterns in the absence of genetic variation. *Genome*
523 *biology* **18**, 155 (2017).
524
525 9. Li Q*, et al.* Genetic Perturbation of the Maize Methylome. *Plant Cell*, (2014).
526
527 10. Hu L*, et al.* Mutation of a major CG methylase in rice causes genome-wide
528 hypomethylation, dysregulated genome expression, and seedling lethality.
529 *Proc Natl Acad Sci U S A* **111**, 10642-10647 (2014).
530
531 11. Tahiliani M*, et al.* Conversion of 5-methylcytosine to 5-
532 hydroxymethylcytosine in mammalian DNA by MLL partner TET1. *Science*
533 **324**, 930-935 (2009).
534
535 12. Pastor WA*, et al.* Genome-wide mapping of 5-hydroxymethylcytosine in
536 embryonic stem cells. *Nature* **473**, 394-397 (2011).
537

538 13. Ito S, D'Alessio AC, Taranova OV, Hong K, Sowers LC, Zhang Y. Role of Tet
539 proteins in 5mC to 5hmC conversion, ES-cell self-renewal and inner cell mass
540 specification. *Nature* **466**, 1129-1133 (2010).
541
542 14. Hollwey E, Watson M, Meyer P. Expression of the C-Terminal Domain of
543 Mammalian TET3 DNA Dioxygenase in Arabidopsis thaliana Induces
544 Heritable Methylation Changes at rDNA Loci. *Advances in Bioscience and*
545 *Biotechnology* **7**, 243-250 (2016).
546
547 15. Erdmann RM, Souza AL, Clish CB, Gehring M. 5-hydroxymethylcytosine is not
548 present in appreciable quantities in Arabidopsis DNA. *G3 (Bethesda)* **5**, 1-8
549 (2014).
550
551 16. Yu M*, et al.* Tet-assisted bisulfite sequencing of 5-hydroxymethylcytosine.
552 *Nature protocols* **7**, 2159-2170 (2012).
553
554 17. Stroud H, Greenberg MV, Feng S, Bernatavichute YV, Jacobsen SE.
555 Comprehensive analysis of silencing mutants reveals complex regulation of
556 the Arabidopsis methylome. *Cell* **152**, 352-364 (2013).
557
558 18. Niederhuth CE*, et al.* Widespread natural variation of DNA methylation
559 within angiosperms. *Genome biology* **17**, 194 (2016).
560
561 19. Saze H, Shiraishi A, Miura A, Kakutani T. Control of genic DNA methylation by
562 a jmjC domain-containing protein in Arabidopsis thaliana. *Science* **319**, 462-
563 465 (2008).
564
565 20. Miura A, Nakamura M, Inagaki S, Kobayashi A, Saze H, Kakutani T. An
566 Arabidopsis jmjC domain protein protects transcribed genes from DNA
567 methylation at CHG sites. *EMBO J* **28**, 1078-1086 (2009).
568
569 21. Rigal M, Kevei Z, Pelissier T, Mathieu O. DNA methylation in an intron of the
570 IBM1 histone demethylase gene stabilizes chromatin modification patterns.
571 *EMBO J* **31**, 2981-2993 (2012).
572
573 22. Lister R*, et al.* Highly integrated single-base resolution maps of the
574 epigenome in Arabidopsis. *Cell* **133**, 523-536 (2008).
575
576 23. Rigal M, Kevei Z, Pélissier T, Mathieu O. DNA methylation in an intron of the
577 IBM1 histone demethylase gene stabilizes chromatin modification patterns.
578 *The EMBO journal* **31**, 2981-2993 (2012).
579
580 24. Soppe WJ*, et al.* The late flowering phenotype of fwa mutants is caused by
581 gain-of-function epigenetic alleles of a homeodomain gene. *Mol Cell* **6**, 791-
582 802 (2000).
583

584 25. Finnegan EJ, Peacock WJ, Dennis ES. Reduced DNA methylation in
585 Arabidopsis thaliana results in abnormal plant development. *Proceedings of*
586 *the National Academy of Sciences of the United States of America* **93**, 8449-
587 8454 (1996).
588
589 26. Ikeda Y, Kobayashi Y, Yamaguchi A, Abe M, Araki T. Molecular basis of late-
590 flowering phenotype caused by dominant epi-alleles of the FWA locus in
591 Arabidopsis. *Plant & cell physiology* **48**, 205-220 (2007).
592
593 27. Baubec T, Finke A, Scheid OM, Pecinka A. Meristem‐specific expression of
594 epigenetic regulators safeguards transposon silencing in Arabidopsis. *EMBO*
595 *reports* **15**, 446-452 (2014).
596
597 28. An YQ, McDowell JM, Huang S, McKinney EC, Chambliss S, Meagher RB.
598 Strong, constitutive expression of the Arabidopsis ACT2/ACT8 actin subclass
599 in vegetative tissues. *The Plant Journal* **10**, 107-121 (1996).
600
601 29. Choudhury SR, Cui Y, Lubecka K, Stefanska B, Irudayaraj J. CRISPR-dCas9
602 mediated TET1 targeting for selective DNA demethylation at BRCA1
603 promoter. *Oncotarget*, (2016).
604
605 30. Maeder ML*, et al.* Targeted DNA demethylation and activation of endogenous
606 genes using programmable TALE-TET1 fusion proteins. *Nat Biotechnol* **31**,
607 1137-1142 (2013).
608
609 31. Vojta A*, et al.* Repurposing the CRISPR-Cas9 system for targeted DNA
610 methylation. *Nucleic Acids Res*, (2016).
611
612 32. Mendenhall EM*, et al.* Locus-specific editing of histone modifications at
613 endogenous enhancers. *Nat Biotechnol* **31**, 1133-1136 (2013).
614
615 33. Liu XS*, et al.* Editing DNA Methylation in the Mammalian Genome. *Cell* **167**,
616 233-247 e217 (2016).
617
618 34. Heard E, Martienssen RA. Transgenerational epigenetic inheritance: myths
619 and mechanisms. *Cell* **157**, 95-109 (2014).
620
621 35. Clough SJ, Bent AF. Floral dip: a simplified method for Agrobacterium-
622 mediated transformation of Arabidopsis thaliana. *The Plant journal : for cell*
623 *and molecular biology* **16**, 735-743 (1998).
624
625 36. Urich MA, Nery JR, Lister R, Schmitz RJ, Ecker JR. MethylC-seq library
626 preparation for base-resolution whole-genome bisulfite sequencing. *Nature*
627 *protocols* **10**, 475-483 (2015).
628

629 37. Martin M. Cutadapt removes adapter sequences from high-throughput
630 sequencing reads. *EMBnet journal* **17**, pp. 10-12 (2011).
631
632 38. Bolger AM, Lohse M, Usadel B. Trimmomatic: a flexible trimmer for Illumina
633 sequence data. *Bioinformatics* **30**, 2114-2120 (2014).
634
635 39. Schmitz RJ*, et al.* Epigenome-wide inheritance of cytosine methylation
636 variants in a recombinant inbred population. *Genome research* **23**, 1663-
637 1674 (2013).
638
639 40. Kim D, Pertea G, Trapnell C, Pimentel H, Kelley R, Salzberg SL. TopHat2:
640 accurate alignment of transcriptomes in the presence of insertions, deletions
641 and gene fusions. *Genome biology* **14**, R36 (2013).
642
643 41. Trapnell C*, et al.* Transcript assembly and quantification by RNA-Seq reveals
644 unannotated transcripts and isoform switching during cell differentiation.
645 *Nature biotechnology* **28**, 511-515 (2010).
646
647 42. Schultz MD, Schmitz RJ, Ecker JR. 'Leveling' the playing field for analyses of
648 single-base resolution DNA methylomes. *Trends in genetics : TIG* **28**, 583-585
649 (2012).
650
651 43. Schultz MD*, et al.* Human body epigenome maps reveal noncanonical DNA
652 methylation variation. *Nature* **523**, 212-216 (2015).
653
654 44. Quinlan AR, Hall IM. BEDTools: a flexible suite of utilities for comparing
655 genomic features. *Bioinformatics* **26**, 841-842 (2010).
656
657
658

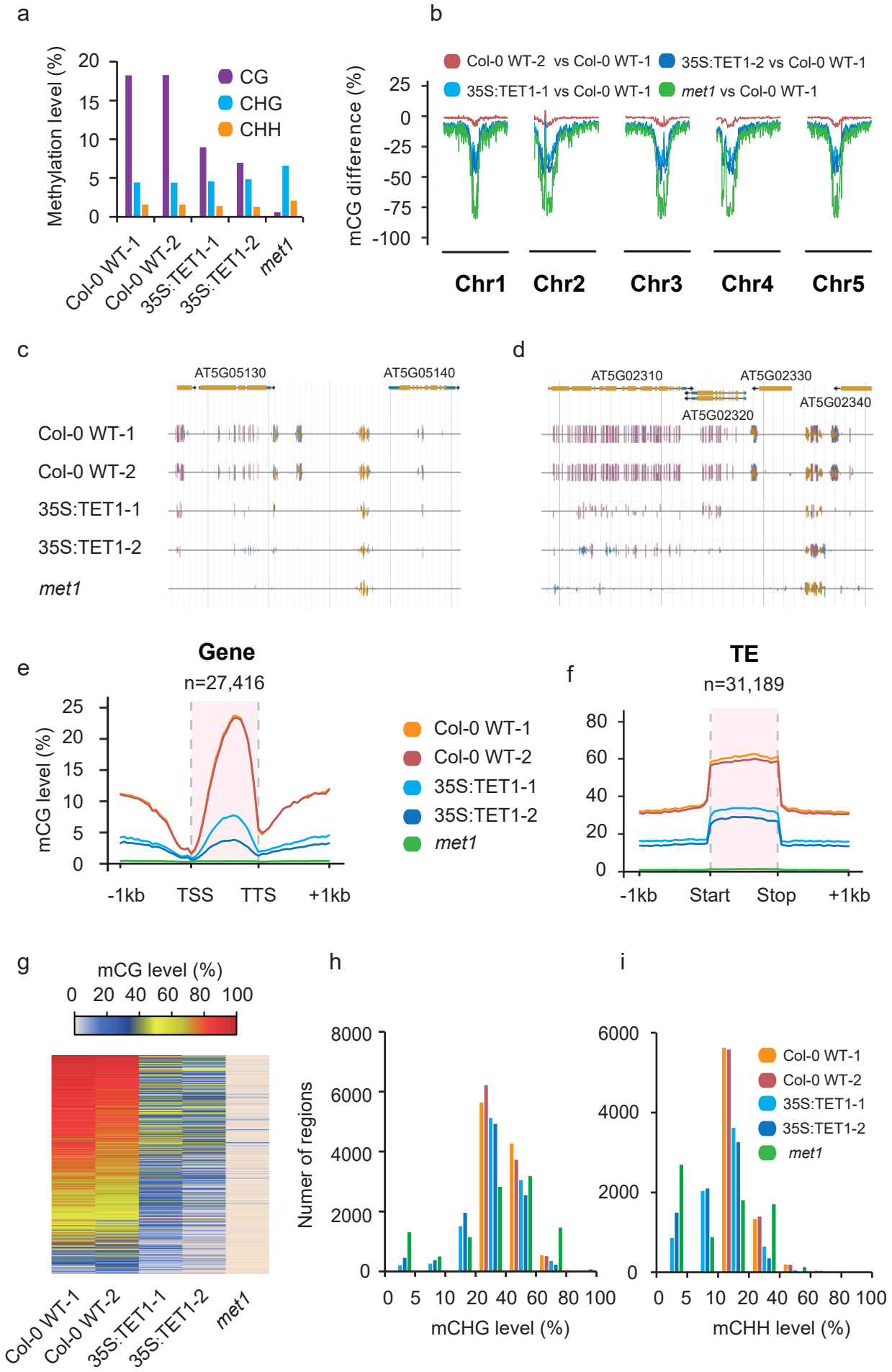
a
Methylation level (%)
20
15
10
5
0
CG
CHG
CHH
Col-0 WT-1
Col-0 WT-2
35S:TET1-1
35S:TET1-2
met1
b
mCG difference (%)
25
0
-25
-50
-75
-100
Col-0 WT-2 vs Col-0 WT-1
35S:TET1-2 vs Col-0 WT-1
35S:TET1-1 vs Col-0 WT-1
met1 vs Col-0 WT-1
Chr1
Chr2
Chr3
Chr4
Chr5
c
AT5G05130
AT5G05140
Col-0 WT-1
Col-0 WT-2
35S:TET1-1
35S:TET1-2
met1
d
AT5G02310
AT5G02330
AT5G02320
AT5G02340
e
Gene
n=27,416
mCG level (%)
25
20
15
10
5
0
-1kb
TSS
TTS
+1kb
Col-0 WT-1
Col-0 WT-2
35S:TET1-1
35S:TET1-2
met1
f
TE
n=31,189
80
60
40
20
0
-1kb
Start
Stop
+1kb
g
mCG level (%)
0 20 40 60 80 100
Col-0 WT-1
Col-0 WT-2
35S:TET1-1
35S:TET1-2
met1
h
Numer of regions
8000
6000
4000
2000
0
0 5 10 20 40 60 80 100
mCHG level (%)
i
6000
4000
2000
0
0 5 10 20 40 60 80 100
mCHH level (%)
Col-0 WT-1
Col-0 WT-2
35S:TET1-1
35S:TET1-2
met1

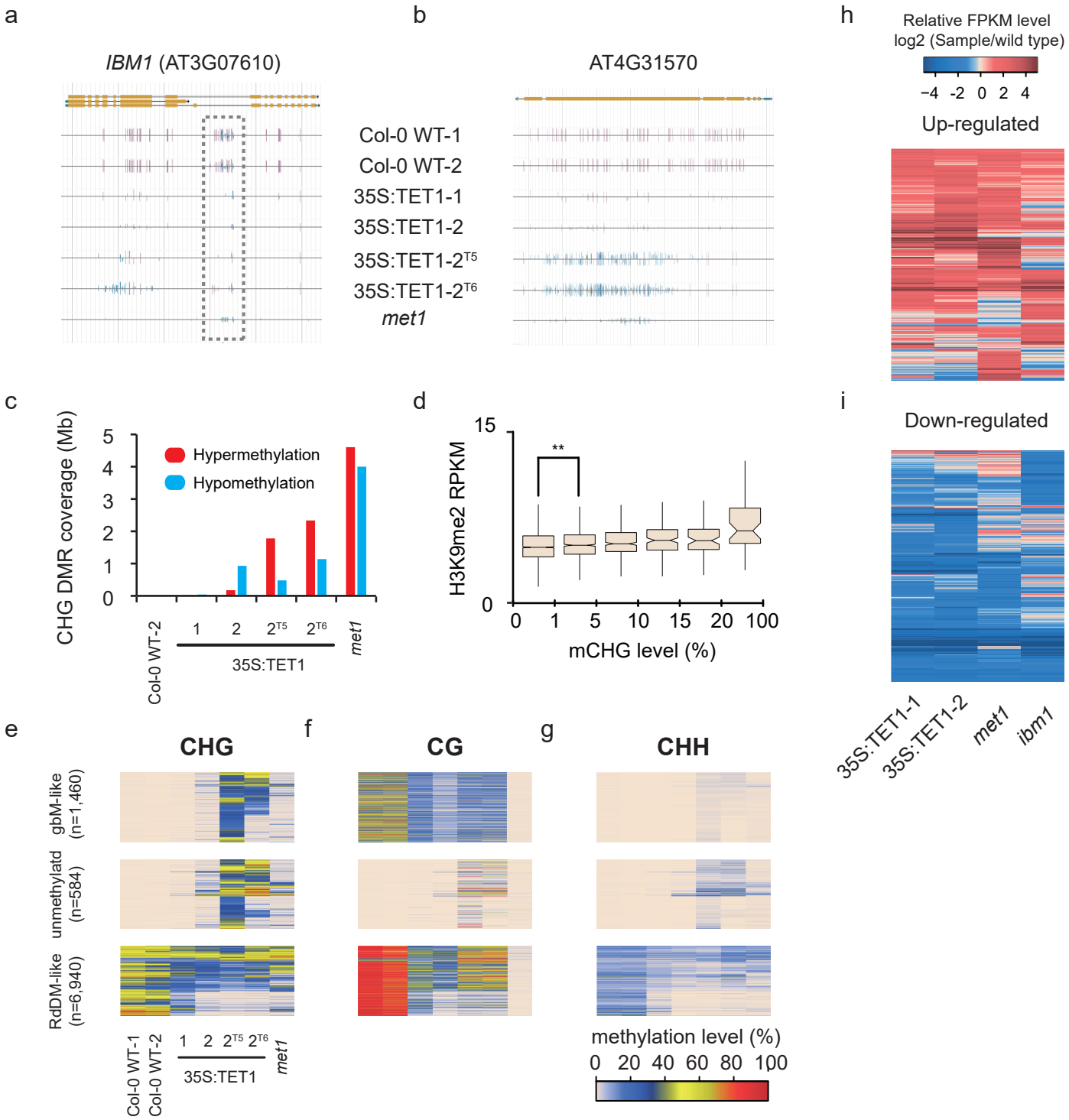
a
IBM1 (AT3G07610)
b
AT4G31570
Col-0 WT-1
Col-0 WT-2
35S:TET1-1
35S:TET1-2
35S:TET1-2T5
35S:TET1-2T6
met1
h
Relative FPKM level
log2 (Sample/wild type)
−4 -2 0 2 4
Up-regulated
c
CHG DMR coverage (Mb)
Hypermethylation
Hypomethylation
Col-0 WT-2
1 2 2T5 2T6
35S:TET1
met1
d
H3K9me2 RPKM
mCHG level (%)
0 1 5 10 15 20 100
i
Down-regulated
35S:TET1-1
35S:TET1-2
met1
ibm1
e
CHG
f
CG
g
CHH
gbM-like (n=1,460)
unmethylatd (n=584)
RdDM-like (n=6,940)
Col-0 WT-1
Col-0 WT-2
1 2 2T5 2T6
35S:TET1
met1
methylation level (%)
0 20 40 60 80 100

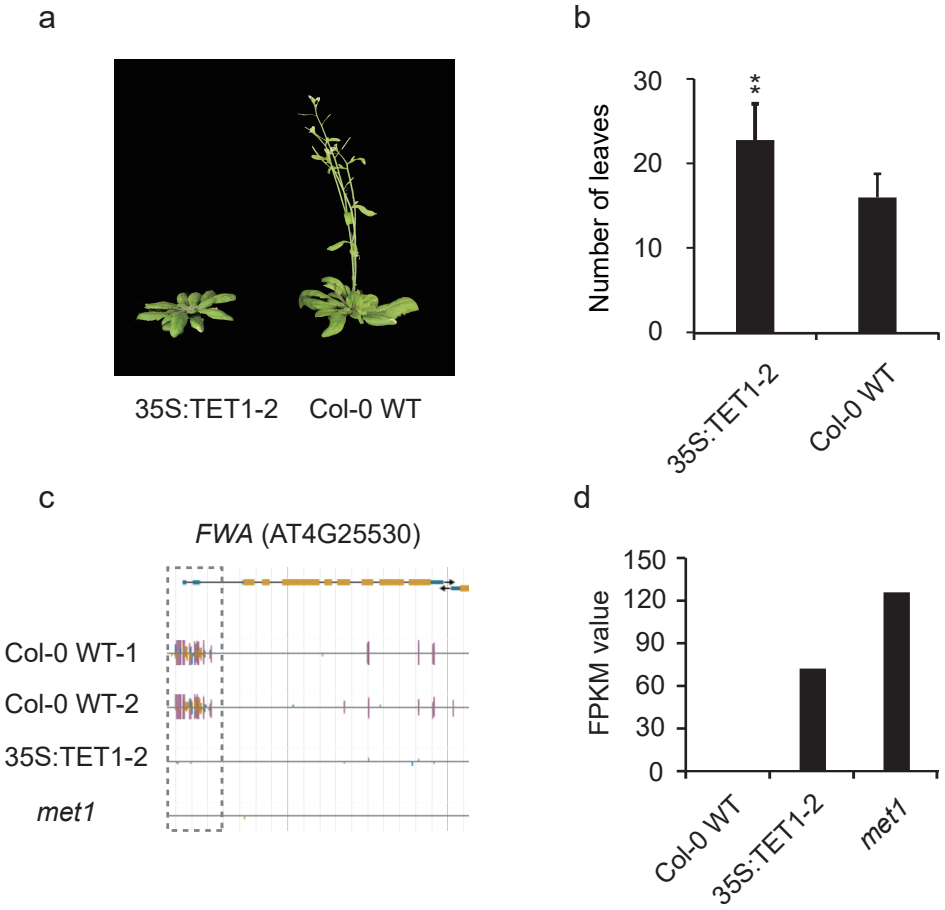
a
35S:TET1-2
Col-0 WT
b
Number of leaves
30
20
10
0
**
35S:TET1-2
Col-0 WT
c
FWA (AT4G25530)
Col-0 WT-1
Col-0 WT-2
35S:TET1-2
met1
d
FPKM value
150
120
90
60
30
0
Col-0 WT
35S:TET1-2
met1

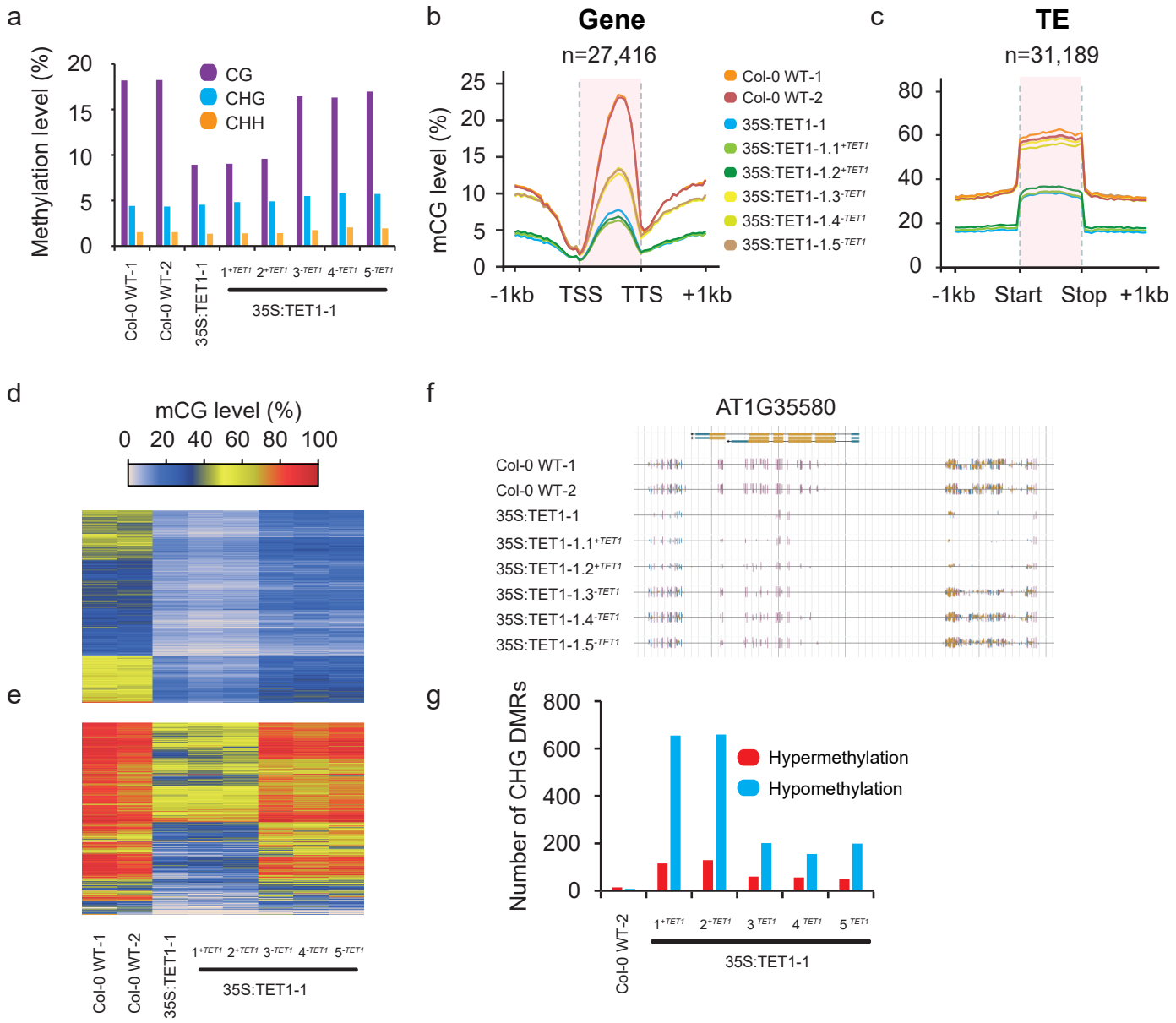
a
Methylation level (%)
CG
CHG
CHH
Col-0 WT-1
Col-0 WT-2
35S:TET1-1
1+TET1 2+TET1 3-TET1 4-TET1 5-TET1
35S:TET1-1
b
Gene
n=27,416
mCG level (%)
Col-0 WT-1
Col-0 WT-2
35S:TET1-1
35S:TET1-1.1+TET1
35S:TET1-1.2+TET1
35S:TET1-1.3-TET1
35S:TET1-1.4-TET1
35S:TET1-1.5-TET1
-1kb TSS TTS +1kb
c
TE
n=31,189
-1kb Start Stop +1kb
d
mCG level (%)
0 20 40 60 80 100
e
Col-0 WT-1
Col-0 WT-2
35S:TET1-1
1+TET1 2+TET1 3-TET1 4-TET1 5-TET1
35S:TET1-1
f
AT1G35580
Col-0 WT-1
Col-0 WT-2
35S:TET1-1
35S:TET1-1.1+TET1
35S:TET1-1.2+TET1
35S:TET1-1.3-TET1
35S:TET1-1.4-TET1
35S:TET1-1.5-TET1
g
Number of CHG DMRs
Hypermethylation
Hypomethylation
Col-0 WT-2
1+TET1 2+TET1 3-TET1 4-TET1 5-TET1
35S:TET1-1

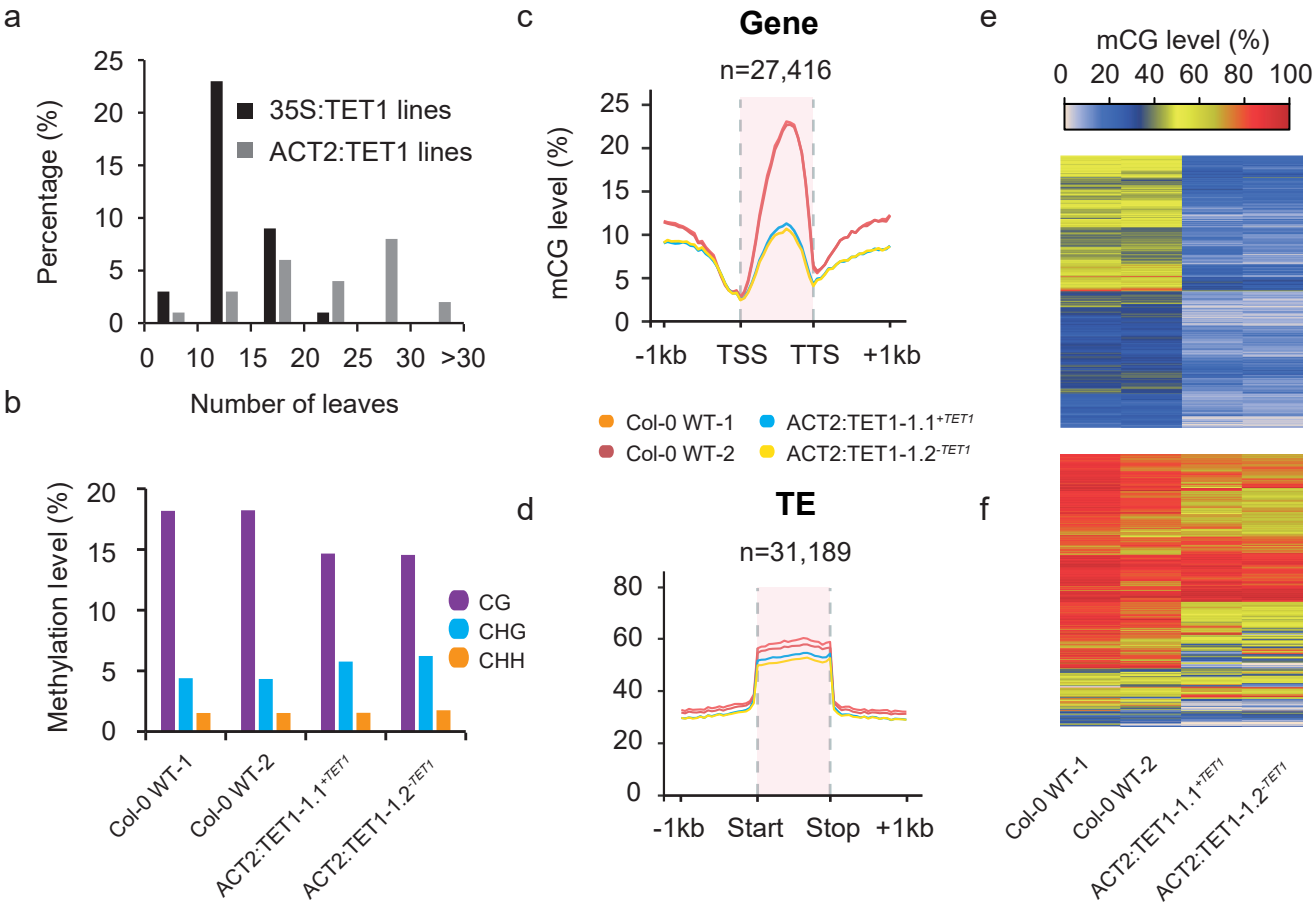
a
Percentage (%)
35S:TET1 lines
ACT2:TET1 lines
Number of leaves
b
Methylation level (%)
CG
CHG
CHH
Col-0 WT-1
Col-0 WT-2
ACT2:TET1-1.1+TET1
ACT2:TET1-1.2-TET1
c
Gene
n=27,416
mCG level (%)
-1kb
TSS
TTS
+1kb
Col-0 WT-1
Col-0 WT-2
ACT2:TET1-1.1+TET1
ACT2:TET1-1.2-TET1
d
TE
n=31,189
-1kb
Start
Stop
+1kb
e
mCG level (%)
f